J|A|C|S ARTICLES

Published on Web 10/29/2010

Mechanistic and Computational Study of a Palladacycle-Catalyzed Decomposition of a Series of Neutral Phosphorothioate Triesters in Methanol

C. Tony Liu, Christopher I. Maxwell, David R. Edwards, Alexei A. Neverov, Nicholas J. Mosey,* and R. Stan Brown*

Department of Chemistry, Queen's University, Kingston, Ontario, Canada K7L 3N6

Received August 9, 2010; E-mail: nicholas.mosey@chem.queensu.ca; rsbrown@chem.queensu.ca

Abstract: The methanolytic cleavage of a series of *O*,*O*-dimethyl *O*-aryl phosphorothioates (**1a**−**g**) catalyzed by a *C*,*N*-palladacycle, (2-[*N*,*N*-dimethylamino(methyl)phenyl]-C^1,N)(pyridine) palladium(II) triflate (**3**), at 25 °C and $^{s}_{s}$pH 11.7 in methanol is reported, along with data for the methanolytic cleavage of **1a**−**g**. The methoxide reaction gives a linear log k_2^{-OMe} vs $^{s}_{s}pK_a$ (phenol leaving group) Brønsted plot having a gradient of $\beta_{lg} = -0.47 \pm 0.03$, suggesting about 34% cleavage of the P−OAr bond in the transition state. On the other hand, the **3**-catalyzed cleavage of **1** gives a Brønsted plot with a downward break at $^{s}_{s}pK_a$ (phenol) $\sim$ 13, signifying a change in the rate-limiting step in the catalyzed reaction, with the two wings having β_{lg} values of 0.0 ± 0.03 and -1.93 ± 0.06. The rate-limiting step for good substrates with low leaving group $^{s}_{s}pK_a$ values is proposed to be substrate/pyridine exchange on the palladacycle, while for substrates with poor leaving groups, the rate-limiting step is a chemical one with extensive cleavage of the P−OAr bond. DFT calculations support this process and also identify two intermediates, namely, one where substrate/pyridine interchange has occurred to give the palladacycle coordinated to substrate through the S═P linkage and to methoxide (**6**) and another where intramolecular methoxide attack has occurred on the P═S unit to give a five-coordinate phosphorane (**7**) doubly coordinated to Pd via the S$^-$ and through a bridging methoxide linked to P and Pd. Attempts to identify the existence of the phosphorane by ^{31}P NMR in a d_4-methanol solution containing 10 mM each of **3**, trimethyl phosphorothioate (a very slow cleaving substrate), and methoxide proved unsuccessful, instead showing that the phosphorothioate was slowly converted to trimethyl phosphate, with the palladacycle decomposing to Pd^0 and free pyridine. These results provide the first reported example where a palladacycle-promoted solvolysis reaction exhibits a break in the Brønsted plot signifying at least one intermediate, while the DFT calculations provide further insight into a more complex mechanism involving two intermediates.

1. Introduction

Sulfur-containing organophosphate triesters containing the P═S group such as fenitrothion (**1c**) and diazinon (**2**) are potent insecticides that inhibit cholinesterases that are essential for neurotransmission. Due to their relatively lower mammalian toxicity, these organophosphates have been widely produced and used,[1] but the possible health and ecological threats due to environmental accumulation necessitate development of effective methods for their bulk destruction and decontamination using efficient chemical means.

We previously reported that $(La^{3+})_2(^{-}OMe)_x$ ($x = 2-5$) and some Zn(II):($^{-}OCH_3$) complexes are very efficient at catalyzing the methanolysis of P═O phosphate triesters,[2] but the former does not decompose P═S triesters in methanol solvent. By contrast, catalysts containing softer metal ions (in the Pearson "Hard/Soft Acid/Base" sense)[3] such as Cu(II) can effectively promote the cleavage of P═S triesters in methanol.[4] Palladacycles bearing a formally Pd(I) soft metal ion, such as **3** and various structural variants, were demonstrated to be efficient catalysts for the cleavage of phosphorothioate triesters in H_2O[5,6] and in MeOH.[7] The process in water, while effective, suffers from problems of poor catalyst solubility and dimerization under basic conditions, as well as product inhibition since the products are phosphorothioate diesters $(RO)_2P(=S)OH$ that bind strongly to the catalyst in their anionic forms.[5,6] Gabbaï has provided important examples whereby the *C*,*N*-palladacycle of phenyloxazoline and a *C*,*N*-2-(2-pyridyl)palladacycle can promote the hydrolysis of methyl parathion (*O*,*O*-dimethyl *O*-*p*-nitrophenyl phosphorothioate, **1**, X = *p*-NO_2) via an intramolecularly

(1) (a) Toy, A. D. F.; Walsh, E. N. In *Phosphorus Chemistry in Everyday Living*, 2nd ed.; American Chemical Society: Washington, DC, 1987; pp 18−20. (b) Quin, L. D. In *A Guide to Organophosphorus Chemistry*; Wiley: New York; 2000; pp 367−371.

(2) (a) Tsang, J. S.; Neverov, A. A.; Brown, R. S. *J. Am. Chem. Soc.* **2003**, *125*, 7602. (b) Tsang, J. S. W.; Neverov, A. A.; Brown, R. S. *Org. Biomol. Chem.* **2004**, *2*, 3457. (c) Desloges, W.; Neverov, A. A.; Brown, R. S. *Inorg. Chem.* **2004**, *43*, 6752. (d) Liu, T.; Neverov, A. A.; Tsang, J. S. W.; Brown, R. S. *Org. Biomol. Chem.* **2005**, *3*, 1525.

(3) Smith, M. B.; March, J. In *Advanced Organic Chemistry*, 5th ed.; Wiley Interscience: New York, 2001; pp 338 and refs cited therein.

(4) Neverov, A. A.; Brown, R. S. *Org. Biomol. Chem.* **2004**, *2*, 2245.

(5) Ryabov, A. D. In *Palladacycles*; Dupont, J., Pfeffer, M., Wiley-VCH: Weinheim; 2008; pp307−339 and references within.

(6) (a) Kim, M.; Liu, Q.; Gabbaï, F. P. *Organometallics* **2004**, *23*, 5560. (b) Kim, M.; Gabbaï, F. P. *Dalton Trans.* **2004**, 3403. (c) Kim, M.; Picot, A.; Gabbaï, F. P. *Inorg. Chem.* **2006**, *45*, 5600.

Scheme 1. Palladacycle (**3**)-Promoted Methanolysis of Phosphorothioates **1**

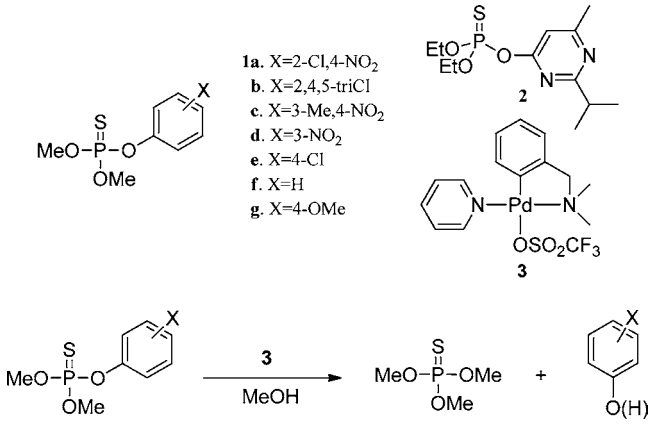

delivered Pd^{-}OH nucleophile within an Pd−S-coordinated complex.[6] For the catalysts studied, a rich chemistry of palladacycle was noted including product bound dimeric and monomeric Pd forms. The methanolytic processes are somewhat simplified because palladacycle **3** is more soluble in alcohol, and catalyst dimerization does not occur. Moreover, since the products are neutral triesters, they bind to the metal ion no more tightly than the substrates and so do not inhibit the catalyst under conditions far from saturation (Scheme 1). The catalysis is very effective: at near neutral $^{s}_{s}$pH = 8.75[8] in MeOH and 25 °C, 1 mM **3** accelerates the methanolytic cleavage of fenitrothion (**1c**) by 4.9×10^9-fold relative to the background $^{-}OCH_3$-promoted reaction.[7d]

Herein, we expand upon the initial investigation[7a] by reporting a comprehensive structure−reactivity study of the catalytic cleavage of a homologous series of dimethyl aryl phosphorothioate triesters **1a**−**g** promoted by **3** in methanol. The results show that, depending on the $^{s}_{s}pK_a$ of the leaving group phenol, the rate of the palladacycle-promoted reaction is limited by different steps in the catalytic cycle, with rate-limiting substrate replacement of pyridine for substrates bearing good leaving groups and rate-limiting cleavage of the P−OAr bond within a palladacycle:substrate complex for substrates with poor leaving groups. This is corroborated by density functional theory (DFT) calculations that also locate an unusually stable five-coordinate phosphorane intermediate bound to the palladacycle along the reaction pathway. All this new information provides valuable insights on how to design more proficient catalysts for the solvolytic cleavage of P═S organophosphate esters.

2. Experimental Section

2.1. Materials and Methods. Sodium methoxide (0.5 M solution in methanol, titrated against N/50 Fisher Certified standard aqueous HCl solution and found to be 0.49 M), $Ag(CF_3SO_3)$, $PdCl_2$ (≥99.9%), 2,2,6,6-tetramethylpiperidine (TMPP) (99+%), dimethyl chlorothiophosphate (98%), 2-chloro-4-nitrophenol (97%), 2,4,5-trichlorophenol (99%), 4-nitrophenol (98%), 4-chlorophenol (99+%), 3-nitrophenol (99%), phenol (99%), 4-methoxyphenol (99%), and 1,8-diazabicyclo[5,4,0]undec-7-ene (98%) were purchased from Aldrich and used without further purification. 1-Methylpiperidine (99%) and 1-ethylpiperidine (99%) were obtained from Alfa Aesar and TCI America Laboratory Chemicals, respectively. $HClO_4$ (70% aqueous solution, titrated to be 12.1 M) and *N*,*N*-dimethylbenzylamine (99%) were purchased from Acros Organics and used as supplied. Anhydrous methanol was acquired from EMD chemicals. Phosphorothioates **1a**−**g** were prepared previously[9] but for this study were synthesized following a published procedure[2d] using dimethyl chlorothiophosphate and the corresponding phenols as the starting materials. The ^{1}H NMR, ^{31}P NMR, and mass spectra obtained are consistent with the structures. Complex **3** was prepared according to a published methodology.[7] *Caution: All the phosphorothioate substrates are acetylcholinesterase inhibitors and should be handled with great care. All glassware and equipment exposed to phosphorothioates should be handled with care using gloves and fume-hood protocols.*

^{1}H NMR and ^{31}P NMR spectra were determined at 400.3 and 162.0 MHz. The $CH_3OH_2^+$ concentrations were determined potentiometrically using a combination glass electrode (Radiometer model XC100-111-120-161) calibrated with certified standard aqueous buffers (pH = 4.00 and 10.00) as described in a previous paper.[10] The $^{s}_{s}$pH values in methanol were obtained by subtracting a correction constant of −2.24[10] from the electrode readings, while the autoprotolysis constant for methanol was taken to be $10^{-16.77}$ M^2. The $^{s}_{s}pK_a$ values of different substituted phenols in methanol can be found in a previous report.[11]

2.2. Kinetics. The kinetic data for the methanolyses of **1** were obtained using either a stopped-flow reaction analyzer (10 mm light path) or conventional UV−vis spectrophotometry at 25 °C. For stopped-flow kinetics, 3 mL stock solutions of catalyst **3** in anhydrous methanol of 0.04 mM < [**3**] < 0.4 mM were prepared in oven-dried vials. The catalyst stock solutions were loaded into one syringe of the stopped-flow analyzer while the other syringe was charged with 0.1 mM **1** and 2 mM 2,2,6,6-tetramethylpiperidine (TMPP) buffer in methanol ($^{s}_{s}pK_a$ = 11.86[7a]). Upon mixing, the final [**3**] ranged from 0.02 to 0.2 mM, [**1**] = 0.05 mM, and [TMPP buffer] = 1 mM. The TMPP buffer was prepared by adding 1/2-equivalent of $HClO_4$ to set the $^{s}_{s}$pH at experimentally measured values of 11.7 ± 0.2. At each catalyst concentration, five consecutive kinetic runs were performed, and the average values of the observed pseudo-first-order rate constants (k_{obs}, obtained by fitting the Abs vs time profiles to a standard exponential equation) were plotted against the [catalyst]. For reactions monitored with conventional UV−vis spectrophotometry, the UV-cells were first charged with 0.05 mM **1** and 1.0 mM TMPP buffer in methanol. The injection of the catalyst initiates the reaction, and the final [**3**] varied from 0.02 to 0.2 mM. The catalyzed reactions were performed in duplicate, and the $^{s}_{s}$pH was controlled at 11.7 ± 0.2 with TMPP buffer as described above. In all cases, the reaction progress was followed by the appearance of the phenolic products of **1a** (393 nm; $\varepsilon = (1.50 \pm 0.03) \times 10^4$ M^{-1} cm^{-1}), **1b** (314 nm; $\varepsilon = (2.6 \pm 0.1) \times 10^3$ M^{-1} cm^{-1}), **1c** (320 nm; $\varepsilon = (4.88 \pm 0.07) \times 10^3$ M^{-1} cm^{-1}), **1d** (330 nm; $\varepsilon = (2.10 \pm 0.06) \times 10^3$ M^{-1}

(7) (a) Lu, Z.-L.; Neverov, A. A.; Brown, R. S. *Org. Biomol. Chem.* **2005**, *3*, 3379. (b) Yang, X.-S.; Long, D.-L.; Li, H.-M.; Lu, Z.-L. *Inorg. Chem. Commun.* **2009**, *12*, 572. (c) Lu, Z.-L.; Yang, X.-S.; Wang, R.-Y.; Fun, H.-K.; Chantrapromma, S. *Polyhedron.* **2009**, *28*, 2565. (d) The acceleration from the cleavage of fenitrothion (ref 7a) is determined as the ratio of the observed pseudo-first-order rate constant for cleavage of fenitrothion by a solution of 1 mM **3** at $^{s}_{s}$pH 8.75 of (k_{cat}^{3} = 35 M^{-1} s^{-1} × (1 × 10^{-3} M **3**) = 3.5 × 10^{-2} s^{-1}) compared with the pseudo-first-order rate constant for the methoxide reaction (7.2 × 10^{-12} s^{-1}) computed from the second-order rate constant for the methoxide reaction (7.2 × 10^{-4} M^{-1}s^{-1}) and the [methoxide = 10^{-8} M] at $^{s}_{s}$pH 8.75.

(8) (a) For the designation of pH in nonaqueous solvents, we use the forms recommended by the IUPAC: *Compendium of Analytical Nomenclature. Definitive Rules 1997*, 3rd ed.: Blackwell: Oxford, U. K., 1998. Since the autoprotolysis constant of MeOH is $10^{-16.77}$, neutral $^{s}_{s}$pH is 8.4. (b) For the description and treatment of "pH" in MeOH, see: Gibson, G.; Neverov, A. A.; Brown, R. S. *Can. J. Chem.* **2003**, *81*, 495.

(9) Kuivalainen, T.; El-Bahraoui, J.; Uggla, R.; Kostiainen, R.; Sundberg, M. R. *J. Am. Chem. Soc.* **2000**, *122*, 8073.

(10) Gibson, G.; Neverov, A. A.; Brown, R. S. *Can. J. Chem.* **2003**, *81*, 495.

(11) Neverov, A. A.; Liu, C. T.; Bunn, S. E.; Edwards, D. R.; White, C. J.; Melnychuk, S. A.; Brown, R. S. *J. Am. Chem. Soc.* **2008**, *130*, 16711.

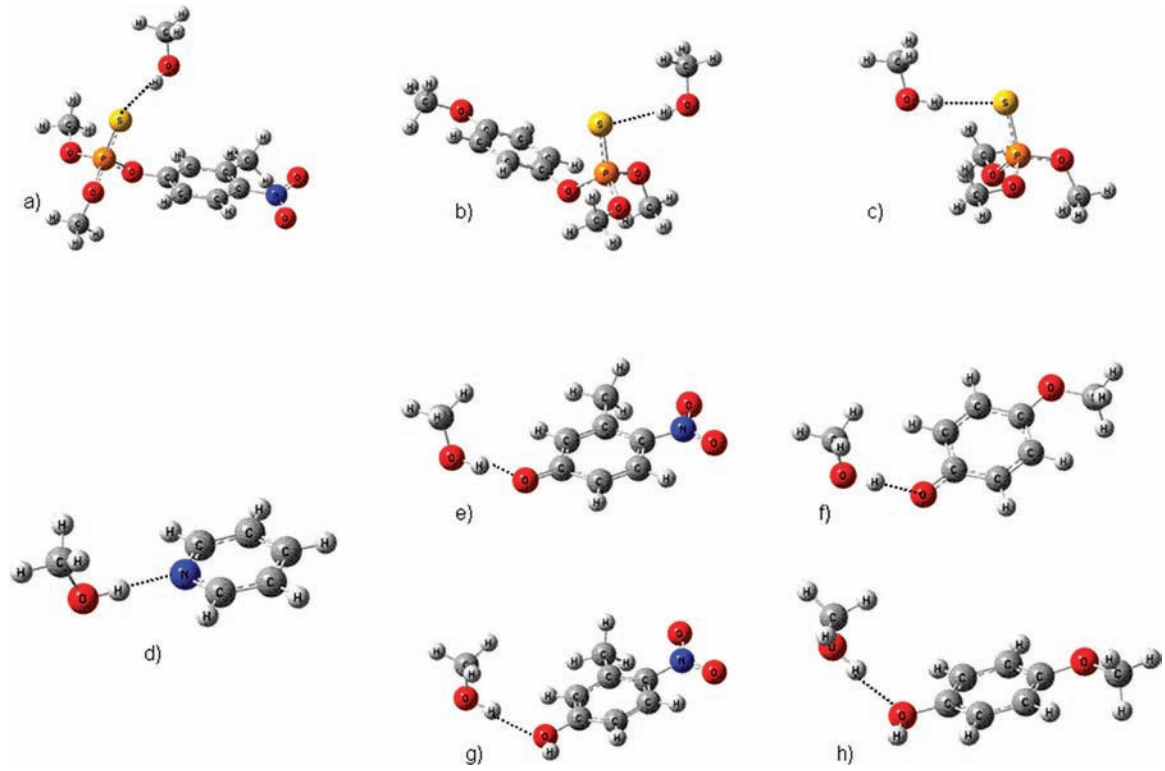

Figure 1. Placement of explicit solvent methanol molecules on nonmetal binding ligands. (a) **1c**, (b) **1g**, (c) $P(S)(OMe)_3$, (d) pyridine, (e) 4-nitro-3-methylphenoxide, (f) 4-methoxyphenoxide, (g) 4-nitro-3-methylphenol, and (h) 4-methoxyphenol.

cm^{-1}), **1e** (284 nm; $\varepsilon = (8.78 \pm 0.02) \times 10^3\ M^{-1}\ cm^{-1}$), **1f** (273 nm; $\varepsilon = (1.76 \pm 0.03) \times 10^3\ M^{-1}\ cm^{-1}$), and **1g** (292 nm; $\varepsilon = (3.28 \pm 0.01) \times 10^3\ M^{-1}\ cm^{-1}$). The absorbance vs time traces exhibit good first-order behavior throughout the full time-course of the reaction in all cases, including when the [catalyst] is less than that of the substrate.[12] It is important to note that even when [catalyst] < [**1**] full release of expected phenolic product was observed so that turnover occurs and there is no product inhibition. The $^{-}OCH_3$-promoted reactions were performed by adding varying amounts of a 1 M stock solution of tetrabutylammonium hydroxide in MeOH so that the [base] ranged from 0.1 to 0.3 M while the [**1**] = 0.1 mM.

2.3. UV−vis Experiments to Determine the Interaction of Palladacycle 3 with Trimethyl Phosphorothioate under Buffered Conditions. A UV−vis cell containing 0.05 mM **3** and 1 mM TMPP buffer in 2.5 mL of methanol was prepared, ^{s}pH 11.6 ± 0.1, 25.0 ± 0.1 °C. To the cell were added aliquots of a 0.5 M stock solution of trimethyl phosphorothioate in methanol, and the UV−vis spectrum (350−200 nm) of the mixture was recorded after each addition. The absorbencies at 255 and 282 nm were corrected for concentration changes and the intrinsic absorbance of trimethyl phosphorothioate in methanol (see Figure 10S, Supporting Information) prior to being plotted against the [trimethyl phosphorothioate] as shown in Figure 3 of the Results section.

2.4. NMR Experiments. ^1H and ^{31}P NMR spectra were recorded at 400.3 and 162.0 MHz, respectively. Stock solutions of catalyst **3** (20 mM), trimethyl phosphorothioate (0.20 M), and $NaOCD_3$ (0.10 M) in CD_3OD were prepared and used to prepare the NMR samples, with the final volume being set at 800 μL with CD_3OD. Phosphoric acid (70% phosphoric acid in H_2O) was used as the reference for ^{31}P NMR.

2.5. Density Functional Theory Calculations. Geometry optimizations and energy calculations of ground and transition states were performed at the B3LYP[13] level of theory using Gaussian 09[14] with the application of the IEFPCM[15] MeOH solvent model. In all calculations, the 6-31G(d,p) basis set was used for C and H atoms, while O, N, P, and S atoms were assigned the 6-31++G(d,p) basis set. The effective core potential of Hay and Wadt with the double-ζ valence basis set (LanL2DZ) was employed to describe Pd.[16] This combination of basis sets was selected after testing several lower and higher levels of theory and finding a good balance of accuracy and speed. Frequency calculations were conducted to characterize transition states and intermediates and to use as a basis for determining free energy values at 298 K.

As ligands dissociate from the complex in solution, they are stabilized by hydrogen bond donors of the solvent. These specific interactions are not included by the IEFPCM solvation model. To account for this stabilization, single explicit solvent molecules were included in some calculations as appropriate, in the form of hydrogen bonding interactions with ligands not included in the complex (Figure 1). Due to the disturbed atom balance in the cases in which the substrate is bidentate-bound, the energy contribution of extra methanol molecules must be included throughout the calculations. When not involved with either the complex or free ligands, these methanol molecules are part of the hydrogen bonded network of the bulk solvent. When free from H-bonding interactions with ligands, methanol is represented by a fractional value of the energy of a PCM solvated methanol hexamer cluster (Figure 2), mimicking the protic environment of a methanol molecule in solution. For instance, one methanol molecule released from

(12) Pseudofirst-order conditions require either that the [catalyst] is at least 10 times larger than substrate or that the concentration of the catalyst [**3**] is constant during the reaction. Since the equilibrium binding of **3** and substrate and its methanolytic product is weak and there is no product inhibition, pseudo-first-order conditions are satisfied since [**3**] remains constant.

(13) (a) Becke, A. D. *Phys. Rev. A* **1988**, *38*, 3098. (b) Lee, C.; Yang, W.; Parr, R. G. *Phys. Rev. B* **1988**, *37*, 785.
(14) Frisch, M. J.; et al. *Gaussian 09*, Revision A.02; Gaussian, Inc.: Wallingford, CT, 2009.
(15) (a) Tomasi, J.; Mennuccia, B.; Cancés, E. *THEOCHEM* **1999**, *464*, 211. (b) Tomasi, J.; Mennuccia, B.; Cammi, R. *Chem. Rev.* **2005**, *105*, 2999.
(16) (a) Hay, P. J.; Wadt, W. R. *J. Chem. Phys.* **1985**, *82*, 270. (b) Wadt, W. R.; Hay, P. J. *J. Chem. Phys.* **1985**, *82*, 284.

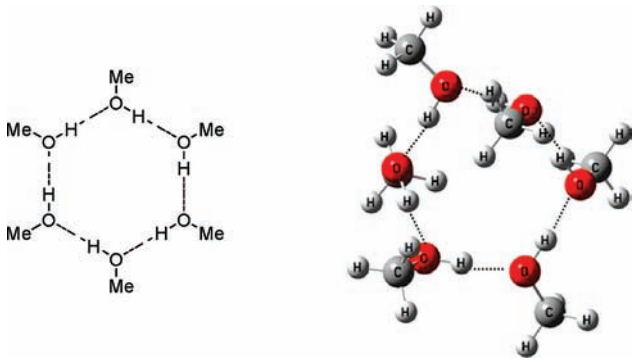

Figure 2. Cyclic hydrogen-bonded methanol hexamer.

H-bonding would be represented as 1/6 of the total energy of the hexamer. A hexamer was used, as there is an increase in dissociation energy per mole of methanol as the size of the cluster increases until it includes six molecules. For clusters of six molecules or more, the dissociation energy per mole of methanol is constant.[17]

The frequency calculations provide access to the free energies evaluated within the ideal gas, rigid rotor, and harmonic oscillator approximations. Such approximations can lead to relative free energies that differ significantly from values obtained in experiments where the systems are solvated. This is particularly true for the bimolecular reactions considered here. These deviations can be traced to an overestimation of the entropic contributions arising from translation and rotational motions. Essentially, the large suppression of these motions in solvent is not captured in the calculations. To correct for this behavior, we follow Sakaki and co-workers[18] and calculate the free energies without including any entropic contributions from translation and rotational motions. Equations 1 and 2 provide a comparison of the standard relative free energy (ΔG) and the definition employed in this work (ΔG_{corr}). The true free energy value would lie between these values, although there are convincing arguments[18] that ΔG_{corr} is more accurate when describing bimolecular processes occurring in solvent.

$$\Delta G = \Delta H - T(\Delta S_{elec} + \Delta S_{trans} + \Delta S_{rot} + \Delta S_{vib}) \quad (1)$$

$$\Delta G_{corr} = \Delta H - T(\Delta S_{elec} + \Delta S_{vib}) \quad (2)$$

2.6. Theoretical ^{31}P NMR Predictions. All molecular geometries were determined using B3LYP and the basis set combination discussed above. Due to inconsistencies[19] in differentiating four- and five-coordinate phosphorus using B3LYP, ^{31}P NMR chemical shifts were predicted at the HF/6-311++G(2d,2p) level of theory using the GIAO formalism.[20] The computed chemical shift of trimethyl phosphorothioate was used as a reference, assigning its chemical shift at the experimental number of 73.26 ppm.

3. Results

3.1. UV−vis Experiments. Shown in Figure 3 is a plot of the change in absorbance at 255 nm that accompanies the addition of trimethyl phosphorothioate to a buffered methanol solution of **3**. The data were treated according to the expression given in eq 3[21] formulated on the basis of the presumed equilibrium given in Scheme 2.

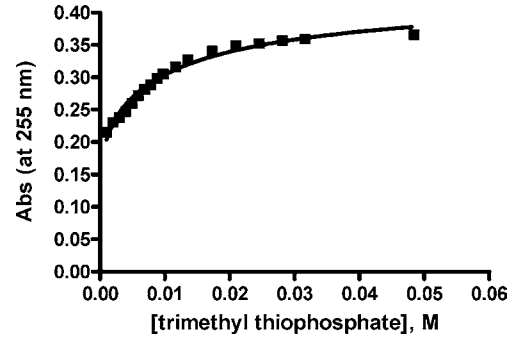

Figure 3. Plot of absorbance at 255 nm vs [trimethyl phosphorothioate] added to a methanol solution of 0.05 mM **3** and 1 mM TMPP buffer at ^{s}pH 11.6 ± 0.1 and 25.0 ± 0.1 °C. The line through the data is calculated for the process given in Scheme 2 for which the equilibrium expression given in eq 3 gives $K = 7.9 \times 10^{-3}$; Abs(int) = 0.13 ± 0.01; and $r^2 = 0.9801$.

Scheme 2. Equilibrium between Palladacycle **3**($^{-}$OCH$_3$) and Trimethyl Phosphorothioate (TMPT) and the Palladacycle-Bound Form of **3**($^{-}$OCH$_3$)(TMPT) Plus Free Pyridine[a]

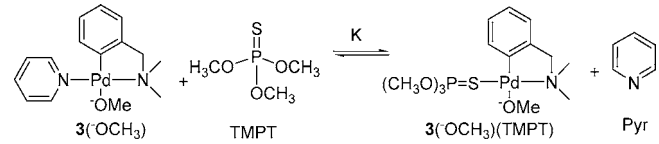

[a] The species labeled as **3**($^{-}$OCH$_3$)(TMPT) is not meant to imply structure, only stoichiometry from the data presented here.

$$\text{Abs} = \text{Ext}_{Pyr}\frac{(-K[\text{TMPT}] + \sqrt{K^2[\text{TMPT}]^2 + 4K[\text{TMPT}][\mathbf{3}(^{-}\text{OCH}_3)]})}{2} + \text{Abs(init)} \quad (3)$$

In eq 3, Ext_{Pyr} refers to the extinction coefficient of pyridine corresponding to the change in absorbance observed at 255 nm, and Abs(init) refers to the absorbance in the absence of added TMPT (see Supporting Information, Figure 10S and footnote 1 on page S6). The so-computed equilibrium constant for the process given in Scheme 2 is $K = 7.9 \times 10^{-3}$.

3.2. Methoxide-Promoted Cleavage of 1a−g. The rates of the base-promoted methanolyses of **1a−g** are linear between 0.1 < [methoxide] < 0.3 M. The second-order rate constants (k_2^{-OMe}) in Table 1 were determined from fitting the k_{obs} vs [methoxide] plots to a standard linear regression, forced through the origin. The Brønsted plot given in Figure 4, constructed from the log k_2^{-OMe} vs ^{s}pK_a values for the parent phenols[11] of the leaving group, has a slope, β_{lg}, of −0.47 ± 0.03.

3.3. Palladacycle 3 Catalyzed Methanolyses of 1a−g. The catalysis exhibited by **3** in methanol is insensitive to the presence of [triflate anion]$_{total}$ up to 2 mM in methanol. We have previously found that **3** tends to decompose slowly over time in basic methanol solutions, forming Pd black or nanoparticles.[2d] Thus, the kinetic experiments here were conducted by preparing a solution of substrate and buffer in methanol, after which the chemical reaction was initiated by adding an appropriate amount of the stock solution of **3**. Under these conditions, buffer

(17) Boyd, S. L.; Boyd, R. J. *J. Chem. Theory Comput.* **2007**, *3*, 54.
(18) (a) Sumimoto, M.; Iwane, N.; Takahama, T.; Sakaki, S. *J. Am. Chem. Soc.* **2004**, *126*, 10457. (b) Tamura, H.; Yamasaki, H.; Sato, H.; Sakaki, S. *J. Am. Chem. Soc.* **2003**, *125*, 16114.
(19) Zhang, Y.; Oldfield, E. *J. Phys. Chem. B.* **2006**, *110*, 579.
(20) Ditchfield, R.; Hehre, W. J.; Pople, J. A. *J. Chem. Phys.* **1972**, *54*, 724.

(21) The equilibrium expression was derived based on the equilibrium process in Scheme 2 while considering the mass balance on Pd catalyst using the commercially available MAPLE software, Maple V Release 5, Waterloo Maple, Inc., Waterloo, Ontario, Canada. $Abs_{(init)}$ is the initial absorbance without any added trimethyl phosphorothioate, and K is the equilibrium constant described in Scheme 2. The path length of the UV-cell used for the spectrophotometric titration is 1 cm.

Table 1. Second-Order Rate Constants for the Base-Promoted (k_2^{-OMe}) and **3**-Catalyzed (k_2^{cat}) Methanolysis of Substrates **1a**−**g** in Methanol, at $T = 25$ °C[a]

Substrate	$^{s}_{s}pK_a$ HOAr	k_2^{-OMe} ($M^{-1}s^{-1}$)	k_2^{cat} ($M^{-1}s^{-1}$)	k_2^{cat}/k_2^{-OMe}
1a	9.35	$(9.3 \pm 0.2) \times 10^{-3}$	1900 ± 50	2.0×10^5
1b	10.73	$(3.9 \pm 0.2) \times 10^{-3}$	1620 ± 40	4.2×10^5
1c	11.50	$(1.05 \pm 0.04) \times 10^{-3}$	2020 ± 60	1.9×10^6
1d	12.41	$(9.1 \pm 0.2) \times 10^{-4}$	1770 ± 20	1.9×10^6
1e	13.59	$(1.22 \pm 0.03) \times 10^{-4}$	565 ± 5	4.7×10^6
1f	14.33	$(5.1 \pm 0.2) \times 10^{-5}$	30.0 ± 0.5	6.0×10^5
1g	14.77	$(3.5 \pm 0.3) \times 10^{-5}$	4.42 ± 0.07	1.3×10^5

[a] The $^{s}_{s}pK_a$ values[11] of the leaving group phenols and the ratios of k_2^{cat}/k_2^{-OMe} are also included.

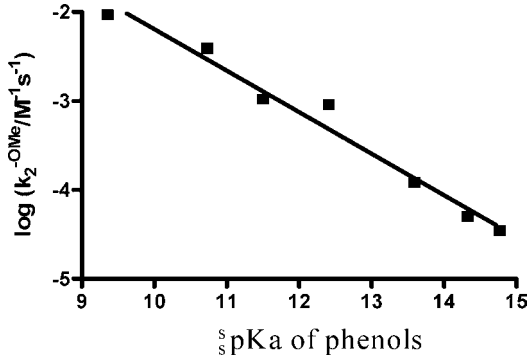

Figure 4. Brønsted plot for the methoxide-promoted cleavages of phosphorothioates **1a**−**g** in methanol at 25.0 ± 0.1 °C. The data points fit a standard linear regression of $\log(k_2^{-OMe}) = (-0.47 \pm 0.03)^{s}_{s}pK_a^{phenol} + (2.5 \pm 0.4)$; $r^2 = 0.9755$.

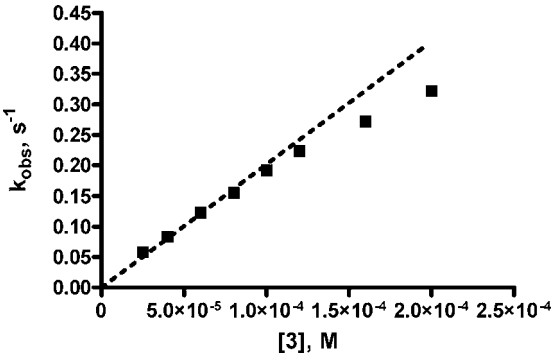

Figure 5. Plot of k_{obs} vs [**3**] for the catalyzed methanolysis of **1c** (5×10^{-5} M) in the presence of 1 mM TMPP at $^{s}_{s}$pH 11.7 ± 0.1 and 25.0 ± 0.1 °C in anhydrous methanol. The linear portion of the data is fitted to a standard linear regression forced through the origin giving $k_2^{cat} = (2020 \pm 60)$ M^{-1} s^{-1}. The ΔAbs (320 nm) values were found to be 0.28 ± 0.01 at the end of the reactions.

catalysis is not observed since the k_{obs} value for the methanolysis of **1c** (0.05 mM) stayed constant at [**3**] = 0.08 mM and 0.3 mM < [TMPP buffer] < 5.0 mM.

The **3**-catalyzed cleavage reactions of **1** were buffered with TMPP at $^{s}_{s}$pH 11.7 ± 0.2, about one $^{s}_{s}$pH unit higher than the reported $^{s}_{s}pK_a$ of 10.8 for the ionization of the Pd-bound methanol to form the Pd-($^{-}OCH_3$) active form of the catalyst.[7] At $^{s}_{s}$pH 11.7, the plots of the first-order rate constant (k_{obs}) for the appearance of the phenolic product vs [**3**] for all substrates were linear to 0.07 mM, and the gradients of each linear portion (see Figure 5 for substrate **1c** and Supporting Information for **1a**,**b**,**d**−**g**) were taken as the second-order rate constants (k_2^{cat}) for the catalyzed reactions; these are given in Table 1. The k_{obs} vs [**3**] data were forced through the origin since the contribution from the methoxide reaction is insignificant in comparison to the catalyzed process. For example, for **1c**, the [$^{-}$OMe] ~ 10^{-5} M at $^{s}_{s}$pH 11.7, which generates a pseudo-first-order rate constant of approximately 1×10^{-8} s^{-1} for the methoxide background reaction. The slight downward curvature observed at higher [**3**] is most likely due to a common species rate depression caused by a small amount of free pyridine, driving a portion of the reactive catalyst:substrate complex back to the free components. As expected, when the reaction is carried out in the presence of excess free pyridine, the downward curvature of the k_{obs} vs [**3**] plots disappears at the expense of reduced reaction rate (Figure 6). In a similar experiment for the cleavage of **1c** (5×10^{-5} M) at a constant [**3**] of 3×10^{-5} M, increasing the added pyridine concentration results in a decrease in the rate of the cleavage of **1c**, and the data can be fit to a common species rate depression equation described in the Supporting Information (Scheme S1 and Figure 7S). These results are discussed in section 4.3.

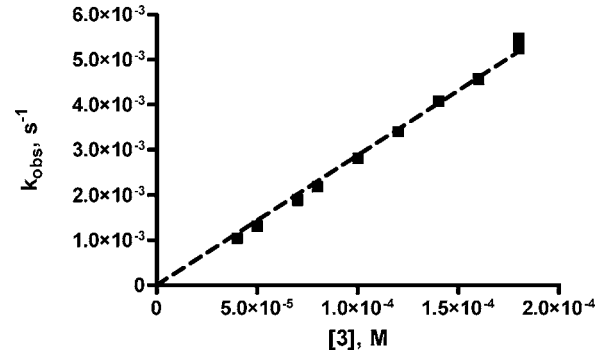

Figure 6. Plot of k_{obs} vs [**3**] for the catalyzed methanolysis of **1c** (5×10^{-5} M) in the presence of 1 mM TMPP buffer and 1.0 mM additional pyridine at $^{s}_{s}$pH 11.6 ± 0.1 and 25.0 ± 0.1 °C in anhydrous methanol. The data are fit to a standard linear regression forced through the origin giving $k_2^{cat} = (28.8 \pm 0.3)$ M^{-1} s^{-1}. The ΔAbs (320 nm) values were found to be 0.28 ± 0.01 at the end of the reactions.

The Brønsted plot of log k_2^{cat} vs $^{s}_{s}pK_a$ (phenol) for the **3**-catalyzed cleavages of **1** shows a clear downward break at $^{s}_{s}pK_a \sim 13$ (Figure 7). The data were treated by nonlinear least-squares (NLLSQ) fitting to an expression[22] for a process where there is a change in rate-limiting step with two β_{lg} values to obtain $\beta_{1(lg)} = 0.00 \pm 0.02$ for the plateau region and $\beta_{2(lg)} = -1.93 \pm 0.06$ for the descending portion.

On the basis of the various kinetic data determined above, we present, in Scheme 3, a working mechanism for the reaction that serves as a model for the DFT calculations that follow.

3.4. DFT Calculations. Calculations were performed for the reaction pathways in Figure 8, which contains a series of structures that are consistent with the mechanism shown in Scheme 3. To explore different domains of the Brønsted plot shown in Figure 7, the calculations were performed for substrates **1c** and **1g**. Figure 8 shows the calculated structures and relevant structural information for the catalytic cleavage of

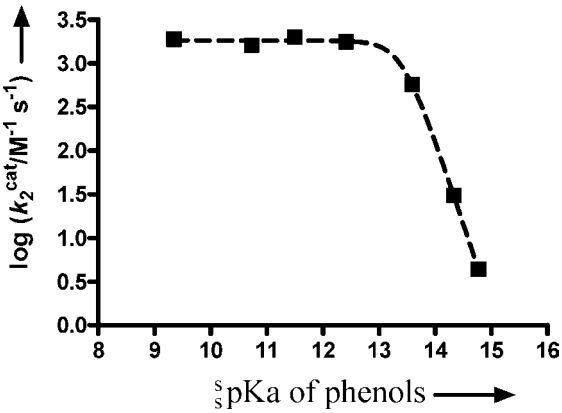

Figure 7. Brønsted plot of log(k_2^{cat}) vs the $^{s}_{s}pK_a$ (phenol) for the **3**-catalyzed cleavage of **1a**−**g** (5×10^{-5} M) in methanol at 25 °C and $^{s}_{s}$pH 11.7 ± 0.2 (1 mM TMPP buffer). The line through the data is generated from a NLLSQ fit to the expression given in ref 22 to provide two β_{lg} values of 0.00 ± 0.02 and −1.93 ± 0.06; $r^2 = 0.9993$.

Scheme 3. Proposed Catalytic Cycle for the Stepwise **3**-Catalyzed Cleavage of **1**

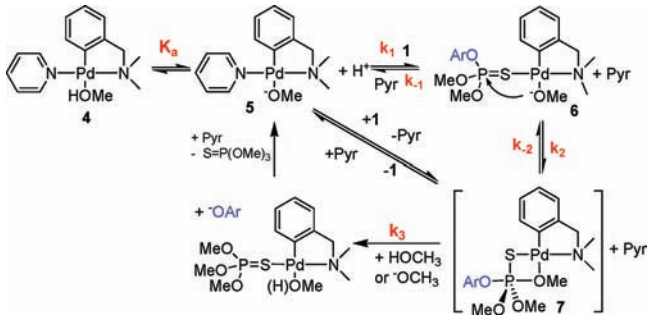

1c. The corrected free energies relative to ground state (ΔG_{corr}), as described in the Experimental Section, do not include the translational and rotational components of the entropy. The ground state (**GS**) geometry has the pyridine in the N-trans position as shown by the X-ray crystal structure of complex **3**.[7a] The ligand exchange process leading from **GS** to $\mathbf{INT_1}$ (**6** in Scheme 3) was modeled as an associative axial attack of the sulfur atom on Pd concurrent with displacement of Pd-bound pyridine through a distorted trigonal−bipyramidal transition state ($\mathbf{TS_{LE}}$). The geometry and bond lengths about the Pd center (see Supporting Information) are similar for both substrates. Stable five-coordinate Pd intermediates including incoming and outgoing ligands could not be located, consistent with what would be expected for a concerted associative[23] ligand exchange on the Pd center. The $\Delta G^{‡}_{corr}$ values for **1c** and **1g** are 10.6 and 8.4 kcal mol^{-1}, respectively, in passing from **GS** to $\mathbf{INT_1}$ which lies in a shallow minimum for both **1c** and **1g**. For both substrates, intramolecular nucleophilic attack of the Pd-bound methoxide proceeds through a transition state $\mathbf{TS_{Nu}}$ with a relative free energy similar to that of the ligand exchange process. Interestingly, the bidentate five-coordinate phosphorane intermediates $\mathbf{INT_2}$ (**7**) are found to be stable species.

Shown in Figure 9 are computed structures, according to the pathway followed in Figure 8, for the methanolysis of **1c** and **1g**. The departure of OAr occurs through a lengthening of the P−OAr bond of $\mathbf{INT_2}$. This barrier is low for **1c** ($\Delta G_{corr} = 5.2$ kcal mol^{-1}). However, a barrier of $\Delta G^{‡}_{corr} = 15.2$ kcal mol^{-1} is required to expel the poorer leaving group of **1g**. This substrate also has a larger calculated P−OAr distance in the transition state (2.87 Å) vs 1.72 Å in $\mathbf{INT_2}$. In both cases, as the P−OAr bond lengthens, the Pd−OMe bond length increases somewhat in the transition state (for **1g**, 2.49 vs 2.26 Å in $\mathbf{INT_2}$) to accommodate the increasingly tetrahedral geometry of the phosphorothioate center (see Table 4S, Supporting Information). This weakened Pd−OMe coordination likely contributes to the eventual dissociation of the trimethyl phosphorothioate product during the turnover process. Upon examination of the overall energy profile in Figure 8 for **1c**, the rate-determining process involves $\mathbf{TS_{LE}}$, and subsequent chemical steps are energetically downhill. With **1g**, the largest energy barrier is associated with the expulsion of the leaving group ($\mathbf{TS_{LG}}$).

3.5. NMR Experiments. The ^{31}P NMR spectra for a sample containing 10 mM **3** and trimethyl phosphorothioate in the absence of added base show only the presence of free trimethyl phosphorothioate with a multiplet for the phosphorus at δ = 73 ppm (Figure 13S Supporting Information). For this sample, the proton NMR reveals peaks associated with the free palladacycle **3** (spectrum not shown). With 5 mM added base, a new phosphorus multiplet at ∼2 ppm was also observed as well as the free phosphorothioate peak at 73 ppm (Figure 19S Supporting Information), the integrated ratio of these being 0.29/1.0. The new ^{31}P peak at ∼2 ppm can be linked to the new P−(OCH$_3$) group at ^{1}H δ = 3.78 ppm through an HMBC experiment. As the concentration of base increases to 10 mM while keeping the [**3**] and [trimethyl phosphorothioate] both at 10 mM, the ratio of the new species (^{31}P δ 2.25 ppm) to the unbound trimethyl phosphorothioate (^{31}P δ 73 ppm) also increases to 1.39/1.0 (see Figure 10 and Figures 14S−18S, Supporting Information). In the Figure 10 spectrum taken after 3 h, there is also a small peak (∼4%) at δ 37.63 which can be shown by spiking to be the Pd-bound form of the dimethyl phosphorothioate anion (compare Figure 14S and 17S, Supporting Information). Addition of up to 3 equiv of methoxide caused the phosphorothioate peak at 73 ppm to be completely transformed into the peak at ∼2 ppm. This peak proved to belong to trimethyl phosphate as proven by spiking the sample with authentic material (Figure 16S Supporting Information).

The ^{31}P chemical shifts of trimethyl phosphorothioate and palladium-bound tetramethyl phosphorane **7** computed using the approach described in section 2.6 above were 73 and −22 ppm, respectively, referenced as described in section 2.6.

4. Discussion

4.1. Methoxide-Promoted Cleavage of 1a−g. The methoxide-promoted methanolyses of phosphorothioates **1a**−**g** show a moderate sensitivity to the nature of the leaving group on the substrate, giving a Brønsted β_{lg} value of −0.47 ± 0.03. This can be compared with the linear Brønsted correlations for the $^{-}$OH-promoted hydrolyses of diethyl aryl phosphate triesters (P=O; $\beta_{lg} = -0.43$)[24] and diethyl aryl phosphorothioate triesters (P=S; $\beta_{lg} = -0.35$)[25] and the methoxide-promoted methanolysis

(22) The NLLSQ equation defined for two β values and a β for equilibrium binding of the catalyst and substrate has the following form

$$k_2^{obs} = K_b k_1 k_2/(k_{-1} + k_2) = C_b C_1 C_2 10^{(\beta_b+\beta_1+\beta_2)pK_a}/(C_{-1}10^{\beta_{-1}pK_a} + C_2 10^{\beta_2 pK_a})$$

presented as eq 3 in: Neverov, A. A.; Sunderland, N. E.; Brown, R. S. *Org. Biomol. Chem.* **2005**, *3*, 65.

(23) (a) Krüger, H.; van Eldik, R. *Chem. Commun.* **1990**, *4*, 330. (b) Holmann, H.; Suvachittanont, S.; van Eldik, R. *Inorg. Chim. Acta* **1990**, *177*, 151.

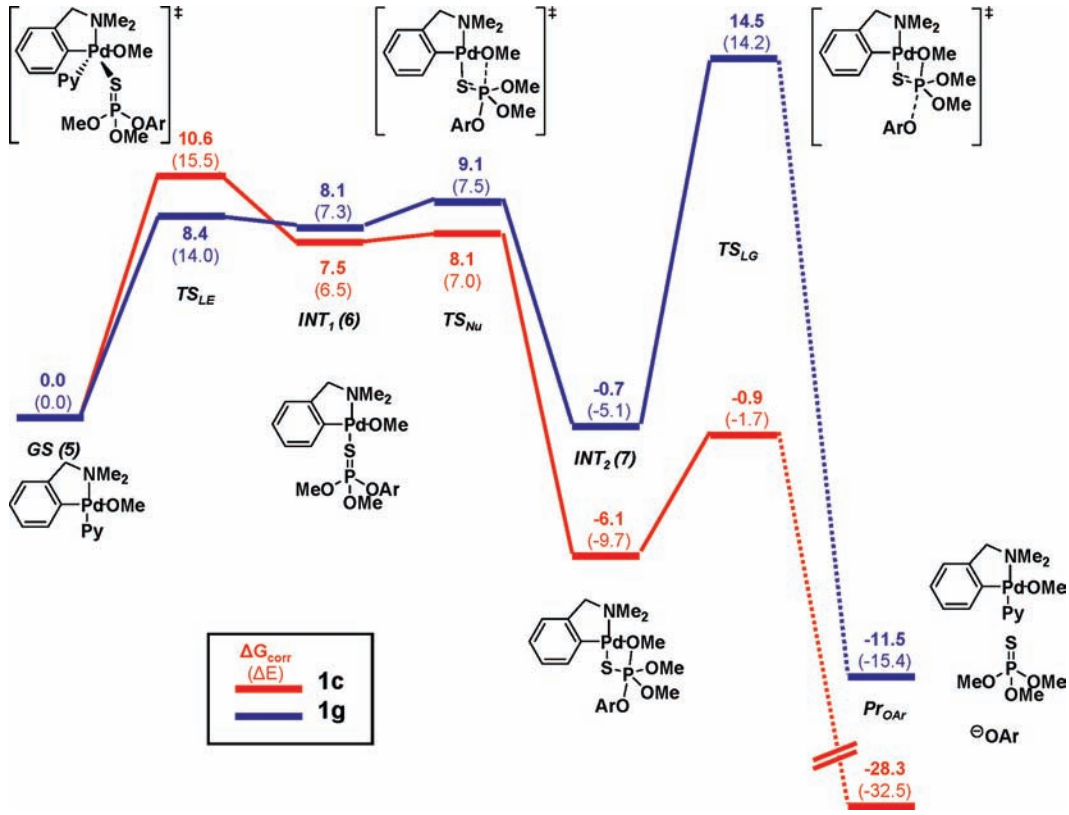

Figure 8. DFT computed reaction pathways (including ΔG_{corr} and ΔE values) for the **3**-catalyzed methanolysis of **1c** (red) and **1g** (blue). Dotted lines corresponding to product dissociation steps are not expected to be kinetically relevant and are currently being investigated. The catalytic products include protonated leaving groups (Pr_{HOAr}, not shown) formed subsequent to the P−OAr cleavage: at the experimental ${}^{s}_{s}$pH of 11.7, **1c** exists ∼50% in its deprotonated form while **1g** exists as the phenol. Plot is to scale.

of diethyl aryl phosphate triesters ($\beta_{lg} = -0.70$).[2d] The lyoxide-catalyzed cleavages of acyclic neutral phosphate triesters[26] and dimethyl aryl phosphorothioate esters such as fenitrothion (**1c**)[27] are considered to be concerted. The β_{eq} value for the equilibrium

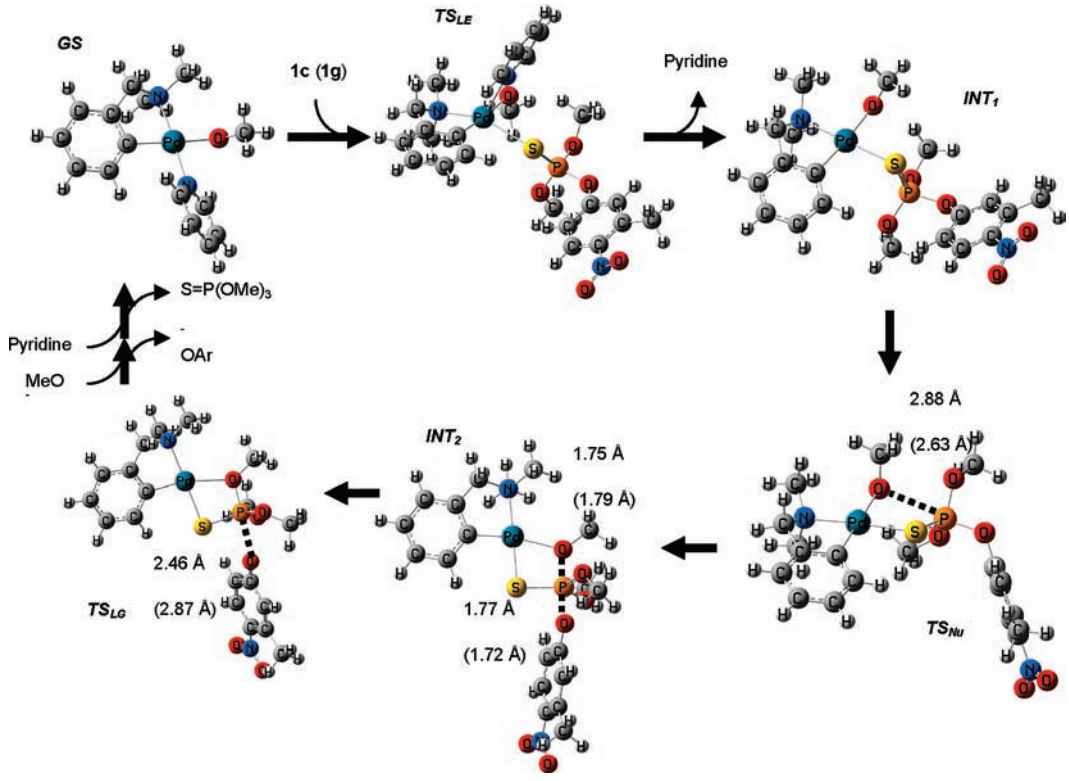

Figure 9. Computed structures for the methanolysis of **1c**. Selected bond lengths are shown with the corresponding value for **1g** in parentheses.

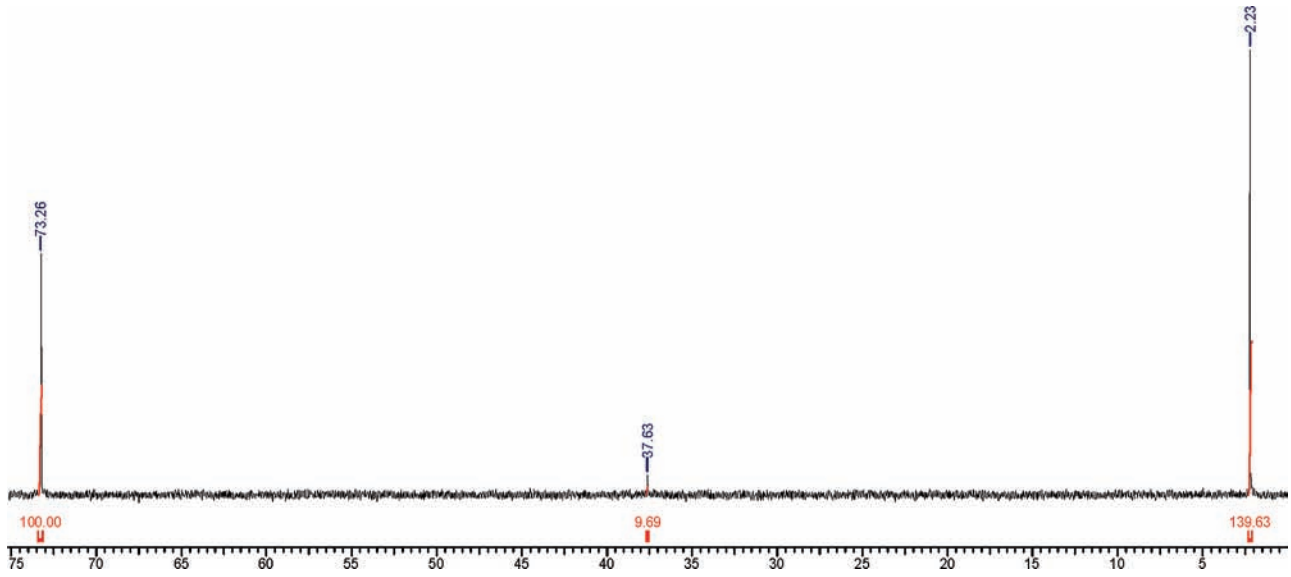

Figure 10. Proton decoupled ^{31}P NMR (162.0 MHz) of a solution containing 10 mM palladacycle **3**, trimethyl phosphorothioate, and $NaOCD_3$ in CD_3OD 3 h after mixing. Integrated ratio of the two peaks at 2.23 ppm and 73.26 ppm is 6:4, while intensity of the peak at 37.63 ppm is ~4% of the total.

transfer of the diethoxy phosphoryl group between oxyanion nucleophiles is reported to be −1.87 in water[28] and results from the change in effective charge on the aryloxy oxygen passing from +0.87 in the starting phosphate to −1 in the phenoxide product. Under the assumption that the β_{eq} value in methanol is similar, the water value was used to calculate the Leffler parameter[29] ($\alpha = \beta_{lg}/\beta_{eq} = -0.70/-1.87 = 37\%$) that is a measure of the extent of P−OAr cleavage for the CH_3O^--promoted methanolysis of P═O triesters. In a study concurrent with this one, we have determined that the β_{eq} value for transfer of the $(MeO)_2P{=}S$ group between oxyanions in water is ~ −1.40,[30] which replaces an earlier value of −0.88.[31] Assuming that the transfer of the reaction from water to methanol does not change the β_{eq} value,[32] the Leffler parameter for cleavage of phosphorothioates is $\alpha = \beta_{lg}/\beta_{eq} = 34\%$, meaning that extent of cleavage of the OAr group from the P═S esters in the transition state is slightly less than that for P═O esters (37%), although consideration of the experimental errors makes the two numbers essentially the same. This finding is complementary to data obtained from ^{18}O and ^{15}N kinetic isotope effect studies indicating that leaving group departure during alkaline hydrolysis of *O,O*-dimethyl *O*-*p*-nitrophenyl phosphorothioate is somewhat less advanced than is the case for phosphate triesters, meaning the transition state is tighter for the former, although the difference between the two types of triesters is not large.[33]

4.2. Palladacycle 3-Catalyzed Cleavage of 1a−g. There are several points of note observed for the **3**-catalyzed cleavage of **1a**−**g** that are consistent with the proposed minimal mechanism presented in Scheme 3. First, the $^{s}_{s}$pH/rate profile for the **3**-catalyzed methanolysis of **1c** has an apparent $^{s}_{s}pK_a$ of 10.8, attributable to the generation of the internal Pd−($^-$OCH$_3$) nucleophile (complex **4** → **5** in Scheme 3) as proposed earlier.[7a] The k_{obs} vs [**3**] plots for the cleavage of phosphates **1** (as in Figure 4) exhibit downward curvature at higher concentrations due to a common species rate depression induced by free pyridine in solution, driving complex **6** back to **5** via k_{-1} as in Scheme 3 (Figure 7S, Supporting Information). These results are consistent with an associative reaction pathway[34] involving displacement of pyridine from **5** by the phosphorothioate to generate an active complex suggested to be **6** or a stoichiometric equivalent (possibly **7**). If ligand exchange on Pd were to proceed via a dissociative mechanism, the k_{obs} should exhibit a square root dependence on [**3**], but this is not observed.

Included in Table 1 are all the second-order rate constants for the methoxide- and palladacycle-catalyzed reactions as well as the k_2^{cat}/k_2^{-OMe} ratios of these which are between 10^5 and 10^6, showing that catalyst **3** is very efficient at decomposing series **1** having a wide range of leaving group ability.

As far as we know, this is the first study of a palladacycle-catalyzed solvolysis of a contiguous series of substrates with

(24) (a) Khan, S. A.; Kirby, A. J. *J. Chem. Soc. (B)* **1970**, 1172. (b) Rowell, R.; Gorenstein, D. G. *J. Am. Chem. Soc.* **1981**, *103*, 5894.
(25) Hong, S.-B.; Raushel, F. M. *Biochemistry* **1996**, *35*, 10904.
(26) Ba-Saif, S. A.; Williams, A. *J. Org. Chem.* **1988**, *50*, 2204.
(27) Omakor, J. E.; Onyido, I.; vanLoon, G. W.; Buncel, E. *J. Chem. Soc., Perkin Trans.* **2001**, *2*, 324.
(28) (a) Ba-Saif, S. A.; Waring., M. A.; Williams, A. *J. Am. Chem. Soc.* **1990**, *112*, 8115. (b) Ba-Saif, S. A.; Waring., M. A.; Williams, A. *J. Am. Chem. Soc.* **1991**, *112*, 1653.
(29) (a) Leffler, J. E.; Grunwald, E. In *Rates and Equilibria of Organic Reactions*; Wiley: New York, 1963. (b) Williams, A. *Acc. Chem. Res.* **1984**, *17*, 425.
(30) A preliminary concurrent study of β_{Nuc} and β_{lg} values for the cleavage of substrates **1** gives a β_{eq} value for the transfer of the $(MeO)_2P{=}S$ group between oxyanion nucleophiles in water of −1.40. Harkness, R.; Edwards, D. E.; Brown, R. S., Unpublished results.
(31) A β_{eq} value for the transfer of the $(MeO)_2P{=}S$ group between oxyanions was reported[27] to be−0.88 as determined from a nonsymmetrical reaction where the incoming nucleophile (phenoxide) has a higher pK_a than any of the substrate electrophiles. This number serves as a lower limit for the actual absolute value of the β_{eq}.
(32) This assumption is reasonable if one considers that the linear free energy plot is log k_2 vs $^{s}_{s}pK_a^{phenol}$ and has the *x*-axis corrected for the pK_a difference of the phenol in water vs methanol. If we were simply plotting the LFE relationship vs σ^--values obtained in water, the the relationship would not be corrected for the effect of solvent (the *r*-value obtained on that solvent). Fortunately, in the case of the $^{s}_{s}pK_a$ values we have used, the *x*-axis incorporates the solvent effect on the ionization of phenol in methanol vs water. We have discussed the applicability of this assumption to the case of phosphotriesters cleaved by a dinuclear phosphotriesterase where very large β_{lg} values are found: Liu, T.; Neverov, A. A.; Tsang, J. S. W.; Brown, R. S. *Org. Biomol. Chem.* **2005**, *3*, 1525.
(33) Catrina, I. E.; Hengge, A. C. *J. Am. Chem. Soc.* **2003**, *125*, 7546.
(34) (a) Krüger, H.; van Eldik, R. *Chem. Commun.* **1990**, *4*, 330. (b) Holmann, H.; Suvachittanont, S.; van Eldik, R. *Inorg. Chim. Acta* **1990**, *177*, 151.

controlled leaving group abilities. As such, it shows a heretofore unexpected feature where the Brønsted plot for **3**-catalyzed cleavage of **1** has a downward break (Figure 7). This sort of break in a linear free-energy plot is consistent with a change in rate-limiting step for the catalyzed reaction which can be described by the minimal form of eq 4 that gives rise (with steady state treatment in **6**) to the expression in eq 5. With good substrates, **1a**−**d**, the process is insensitive to the nature of OAr ($\beta_{lg} = 0.00 \pm 0.02$), while with poor leaving groups (**1e**−**g**) the observed $\beta_{lg} = -1.93 \pm 0.06$, suggestive of a rate-limiting transition state with substantial P−OAr bond scission, is consistent with the DFT calculation of the TS structure for the cleavage of Pd-bound **1g**. The change in

$$\mathbf{5} + \mathbf{1} \underset{k_{-1}}{\overset{k_1}{\rightleftharpoons}} \mathbf{6} + \text{Pyr} \xrightarrow{k_{cat}} \text{P} \tag{4}$$

$$k_{obs} = k_1[\mathbf{1}]/(1 + (k_{-1}/k_{cat})[\text{Pyr}]) \tag{5}$$

the rate-limiting step can be accommodated by the process in Scheme 3 where a step involving substrate exchange for Pd-bound pyridine precedes the chemical step of intramolecular attack of Pd−($^-$OCH$_3$) on the Pd-bound substrate to yield a possible five-coordinate phosphorane intermediate bound to the palladacycle (**7**), followed by P−OAr cleavage. The insensitivity of the Brønsted β_{lg} to the nature of **1a**−**d** with good leaving groups suggests that the substrate−pyridine interchange (k_1) is rate-limiting for reactions of these substrates, and P−OAr scission (k_3) is rate-limiting for **1e**−**g**. We point out that the apparent β_{lg} value of −1.93 for the latter substrates seems large for a simple cleavage of the P−OAr bond and is larger than the limit imposed by the β_{eq} for simple transfer of the (MeO)$_2$P═S group between oxyanion nucleophiles.[30] While more work is underway to investigate the origin of the large β_{lg}, its magnitude is such that considerable departure of the leaving group must occur in the TS. Large values of β_{lg} of −1.43 and −1.12 are also seen for La^{3+} and Zn(II):(1,5,9-triazacyclododecane)-catalyzed methanolyses of neutral phosphate esters, suggesting the rate-limiting TSs for the catalytic methanolysis reactions also have considerable P−OAr cleavage.

4.3. Other Catalytic Mechanistic Considerations. The rather small k_2^{cat} values of $\sim 2 \times 10^3$ M^{-1} s^{-1} for the methanolyses of the fast reacting substrates **1a**−**c** (Table 1) might seem slow for a proposed process that involves ligand exchange on metal centers, as these can be extremely rapid ($(2-20) \times 10^8$ M^{-1} s^{-1})[35] in numerous cases involving transition metals. However, ligand exchange on a Pd(II) center can be much slower.[34,36] The overall process that emerges for the complex-catalyzed cleavage of these phosphorothioates is reminiscent of the enzymatic hydrolysis of phosphate triesters and phosphorothioate triesters by a metallo-phosphotriesterase extracted from the bacterium *Pseudomonas diminuta*.[25,37,38] There, similar biphasic Brønsted plots were obtained where the enzymatic hydrolysis rate constants for substrates with HOAr pK_a < 8 are insensitive to the leaving group ability, while a large leaving group dependency ($\beta = -2.2$ for P═O and $\beta = -2.0$ for P═S) was found for substrates containing OAr groups where the phenols have pK_a values >8.

Scheme 4. Proposed Equilibrium Formation of a Stable Palladacycle-Coordinated Phosphorane (**7$_{OMe}$**) from the Reaction of **5** and Trimethyl Phosphorothioate via the Intermediacy of **6$_{OMe}$**

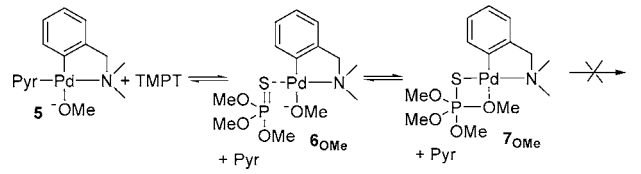

4.4. Density Functional Theory Study. The DFT calculations provide further validation of, and insights into, the proposed mechanism. The reaction pathway suggested in Scheme 3 was computed for a representative substrate from each domain of the Brønsted plot in Figure 7 (**1c** and **1g**). What becomes apparent from Figure 8 is that the highest energy barriers along the reaction pathway for substrates **1c** and **1g** are those for ligand exchange (**TS$_{LE}$**) and leaving group departure (**TS$_{LG}$**), respectively. In other words, the DFT study supports the Brønsted plot in Figure 7 where the computed data also suggest a change in the rate-limiting step of the catalyzed reaction as the substrate's leaving group becomes poorer.

For substrate **1c**, the ligand exchange (**TS$_{LE}$**) on the Pd center requires 10.6 kcal mol^{-1} of $\Delta G^{\ddagger}_{corr}$ and is the step with the highest barrier (Figure 8). The subsequent steps are all energetically downhill. Importantly, the DFT calculations located a bidentate five-coordinate phosphorane intermediate (**INT$_2$**) as a stable entity along the reaction coordinate, although the immediate fate of this in the case of **1c** is product formation. Following the energy pathway for substrate **1g**, a similar bidentate five-coordinated phosphorane intermediate was also found prior to the rate-limiting P−OAr bond fission with $\Delta G^{\ddagger}_{corr}$ of 15.2 kcal mol^{-1}. In that case, **INT$_2$** is surprisingly stable with 9.8 kcal mol^{-1} required to revert to **INT$_1$** and 15.2 kcal mol^{-1} to expel the leaving group. Experimentally, the break in the Brønsted plot (Figure 7) signals the existence of at least one intermediate; however, it would be very difficult to propose the presence of two intermediates (**INT$_1$** and **INT$_2$**) without computational data.

What became apparent during this study is the importance of correctly modeling the solvating medium in studying these chemical reactions in solution. As discussed in the Experimental Section, the rotational and translational contributions to entropy are excluded[18] to determine the corrected free energies of activation ($\Delta G^{\ddagger}_{corr}$). It is reasonable to assume that the molecules are solvated by solvent through weak interactions, restricting some, but definitely not all, of their freedom to translocate or rotate freely. The actual free energies most likely lie between those calculated from eq 1, which includes all components of entropy and the entropically corrected ones from eq 2. Sakaki et al. have argued that the values determined from eq 2 are closer to the true values.[18] The data presented here are consistent with that view, and within experimental error, the $\Delta G^{\ddagger}_{corr}$ values determined for the highest barriers from the DFT calculations (**1c**, 10.6 kcal mol^{-1}; **1g**, 14.5 kcal mol^{-1})[39] are surprisingly

(35) Tobe, M. L.; Burgess, J. In *Inorganic Reaction Mechanisms*; Addison Wesley; Longman Ltd.: New York, 1999; pp 271−333.
(36) (a) Rau, T.; Shoukry, M.; van Eldik, R. *Inorg. Chem.* **1997**, *36*, 1454. (b) Shoukry, A.; Rau, T.; Shoukry, M.; van Eldik, R. *J. Chem. Soc., Dalton Trans.* **1998**, 3105. (c) Salas, G.; Casares, J. A.; Espinet, P. *Dalton Trans.* **2009**, 8413. (d) Shi, T.; Elding, L. I. *Inorg. Chem.* **1997**, *36*, 528.
(37) Donarski, W. J.; Dumas, D. P.; Heitmeyer, D. H.; Lewis, V. E.; Raushel, F. M. *Biochemistry* **1989**, *28*, 4650.
(38) (a) Caldwell, S. R.; Newcomb, J. R.; Schlecht, K. A.; Raushel, F. M. *Biochemistry* **1991**, *30*, 7438. (b) Caldwell, S. R.; Raushel, F. M.; Weiss, P. M.; Cleland, W. W. *Biochemistry* **1991**, *30*, 7444.
(39) Ideal Gas at 1 atm and 298 K.

Scheme 5. Minimal Process Describing the Transformations Occurring during Acquisition of the ^{31}P Spectrum of the Reaction Products Formed from a CD_3OD Solution Containing 10 mM Each of Trimethyl Phosphorothioate, Palladacycle **3**, and $^{-}OCH_3$

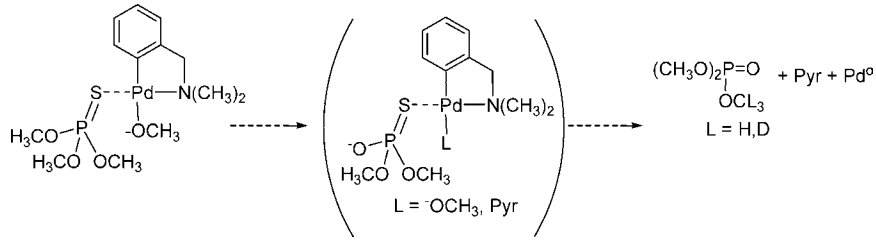

close to those determined experimentally (**1c**, 12.9 kcal mol^{-1}; **1g**, 16.6 kcal mol^{-1}).[40]

It is an apparently surprising consequence that the DFT calculation for the catalyzed cleavage of **1c** (Figure 8) places the Pd-coordinated phosphorane (**7** in Scheme 3) about 8 kcal mol^{-1} lower in energy than its immediate reactant (**6**). It is not immediately clear from the calculation why this is so, but chemical intuition suggests that the stabilization arises from an overall reduction of the magnitude of charges on the S, Pd, and Pd-coordinated methoxy group, transfer of negative charge from the methoxy group to the Pd via increased interaction with the negatively charged thiolate in **7**, and the formation of stronger bonds at the expense of breaking weaker ones. Thus, we speculate that the "hard" methoxy group has a large amount of (−)-charge in **6** which is lessened by the formation of a stronger P−OCH_3 bond in **7** concurrent with the breaking of the P═S bond with transfer of the negative charge to the Pd by way of a prominent "soft−soft" interaction with the S^-. Inspection of the electrostatic potential-derived charges[41] of the Pd, OCH_3, P, and S in the Gaussian optimized $\mathbf{INT_1}$ and $\mathbf{INT_2}$ structures from Figure 8 (see Supporting Information) is consistent with this view.

4.5. Evidence for the Existence of a Palladacycle-Bound Phosphorane 7. An interesting finding from the computational data is the predicted existence of the stable phosphorane **7** along the reaction pathway. This invited an experimental study treating a relatively nonreactive substrate like trimethyl phosphorothioate (TMPT, the initial product of cleavage of **1**) with the palladacycle where the solvolytic breakdown of a putative Pd-coordinated tetramethyl-phosphorane similar to **7** ($\mathbf{7_{OMe}}$ in Scheme 4) would be extremely slow based on the Brønsted correlation and the acidity of methanol in methanol ($^{s}_{s}pK_a$ = 18.2).[42] This may allow one to visualize the putative intermediate by NMR techniques.

At first glance, the −71 ppm upfield chemical shift from δ = 73 ppm for the unbound TMPT to ∼2 ppm (Figure 10) is consistent with the reported chemical shift range (−55 to −85 ppm)[43−45] for neutral and cyclic pentaoxy-phosphoranes and tetraoxy-monothiophosphoranes relative to the neutral four-coordinate phosphorus-containing counterparts. However, the observed 2 ppm peak is without doubt attributable to trimethyl phosphate, as proven by spiking the mixture with authentic material. The exact process by which this is formed is not certain but clearly involves methoxide in transforming the P═S starting material to P═O product, as well as decomposing the palladacycle with the formation of what appears to be Pd^0 nanoparticles as evidenced by a golden brown colored reaction mixture. We do not know the fate of the S once cleaved from trimethyl phosphorothioate, but its loss and the formation of Pd^0 suggest these are involved in redox processes. A minimal process depicting the overall transformation is given in Scheme 5.

5. Conclusions

The results presented here reveal a somewhat different picture for the **3**-catalyzed cleavage of these P═S pesticide models than had been suggested from our previous studies of the single substrate **1c** in methanol[7] and one which might also be operative for the various palladacycle-promoted hydrolyses of these in water.[5,6] This is the first example of a Pd-complex-catalyzed solvolysis of a contiguous series of substrates where a prominent downward break in the Brønsted plot reveals a change in the rate-limiting step of the reaction from substrate binding to breakdown of an intermediate. The latter is suggested to be phosphorane intermediate **7** on the basis of DFT computations which indicates it is formed during the **3**-catalyzed P−OAr cleavage of substrates with both good and poor leaving groups. The experimental and DFT studies provide a complementary picture for the **3**-catalyzed cleavage of phosphorothioates, and we emphasize that the main conclusion that the overall reaction has a change in rate-limiting step involving intermediates **6** and **7** would be difficult to make on experimental or theoretical grounds alone. We note that the catalytic rate constant provided to cleavages of **1** by the basic form of **3** are some (1.3−47) × 10^5 greater than the methoxide-promoted reactions (in terms of k_2^{cat}/k_2^{-OMe}), which points out multiple roles of the metal ion involving substrate activation, perhaps as a Lewis acid, and intramolecular delivery of the coordinated methoxide nucleophile.

The fact that the NMR study did not allow us to provide evidence for the putative palladium-bound phosphorane intermediate is disappointing but does not rule out its existence as an intermediate during the catalytic cleavage of substrates **1**. The test substrate chosen for investigation, trimethyl phosphorothioate, is the product of the very fast cleavage reaction of series **1** and would react extremely slowly if it followed the same pathway as the other substrates **1a**−**g**. From the fit to the Brønsted plot in Figure 7, it would react about 1 million times slower than **1g** with a predicted k_2^{cat} of 1.5 × 10^{-6} M^{-1} s^{-1}. The results of the NMR study indicate that an alternative reaction occurs whereby methoxide and the palladacycle are involved in converting the TMPT to trimethyl phosphate, with the concomitant destruction of the palladacycle to form free pyridine and Pd^0.

The results of this study also suggest that more proficient catalysts might be prepared through structural tuning of complex **3** by replacing the pyridine with a weaker bound ligand to lower the energetic barrier for substrate−ligand exchange on the Pd. This seems to be the only practical method to increase the

(40) Standard State at 1 M and 298 K.
(41) (a) Breneman, C. M.; Wiberg, K. B. *J. Comput. Chem.* **1990**, *11*, 361. (b) Leach, A. R., *Molecular Modelling Principles and Applications*, 2nd ed.; Pearson Education Limited: Harlow, England, 2001; pp 189−191. (c) Bayly, C. I.; Cieplak, P.; Cornell, W. D.; Kollman, P. A. *J. Phys. Chem.* **1993**, *97*, 10269.
(42) Based on the autoprotolysis constant for methanol ($10^{-16.77}$ M^2) and [methanol] in pure solvent.

catalytic decomposition of substrates with good leaving groups, bearing in mind that these are the ones which are commercially important as pesticides.[46] Current work in this lab is focused on the influence of the *C*,*N*-binding ligand and other pyridines in the prepared Pd complex to develop more efficient catalysts in a rational manner. Other aspects of the mechanism, such as the steps leading to catalyst regeneration and the nature of the large negative β_{lg} seen for substrates with poor leaving groups, are also under investigation and will be reported in due course.

(43) (a) Quin, L. D. In *A Guide to Organophosphorus Chemistry*; Wiley: New York, 2000; pp 341−342. (b) Timosheva, N. V.; Chandrasekaran, A.; Holmes, R. R. *Inorg. Chem.* **2006**, *45*, 10836. (c) Holmes, R. R. *Acc. Chem. Res.* **2004**, *37*, 746. (d) Zhang, Y.; Oldfield, E. *J. Phys. Chem. B* **2006**, *110*, 579.
(44) Sherlock, D. J.; Chandrasekaran, A.; Day, R. O.; Holmes, R. R. *Inorg. Chem.* **1997**, *36*, 5082.
(45) Garrossian, M.; Bentrude, W. G.; Röschenthaler, G.-V. *J. Org. Chem.* **2001**, *66*, 6181.
(46) Main, R. A.; Iverson., F. *Biochem. J.* **1966**, *100*, 525.

Acknowledgment. The authors gratefully acknowledge the financial support of NSERC, Canada, and the U.S. Defense Threat Reduction Agency-Joint Science and Technology Office, Basic and Supporting Sciences Division, through the award of grant # HDTRA-08-1-0046. In addition, CTL thanks NSERC for a PGS-2 postgraduate scholarship, and CIM thanks the Ontario Graduate Scholarship. We are also indebted to the High Performance Computing Virtual Laboratory (HPCVL) for their facilities.

Supporting Information Available: Descriptions of experiments and results obtained for various kinetics and for identifying intermediates, ^{31}P NMR spectra for attempts to identify phosphorane, DFT structures and tables of data, CHelpG charges on various atoms in $\mathbf{INT_1}$ and $\mathbf{INT_2}$ structures for **1a** and **1g**, and optimized structure coordinates. Full authorship for ref 14 can be found on page S12. This material is available free of charge via the Internet at http://pubs.acs.org.

JA107144C